JOURNAL OF GEOPHYSICAL RESEARCH, VOL. 113, E11010, doi:10.1029/2008JE003155, 2008

Degradation of Victoria crater, Mars

John A. Grant,[1] Sharon A. Wilson,[1] Barbara A. Cohen,[2] Matthew P. Golombek,[3] Paul E. Geissler,[4] Robert J. Sullivan,[5] Randolph L. Kirk,[4] and Timothy J. Parker[3]

Received 28 March 2008; revised 2 July 2008; accepted 20 August 2008; published 18 November 2008.

[1] The ~750 m diameter and ~75 m deep Victoria crater in Meridiani Planum, Mars, is a degraded primary impact structure retaining a ~5 m raised rim consisting of 1–2 m of uplifted rocks overlain by ~3 m of ejecta at the rim crest. The rim is 120–220 m wide and is surrounded by a dark annulus reaching an average of 590 m beyond the raised rim. Comparison between observed morphology and that expected for pristine craters 500–750 m across indicates that the original, pristine crater was close to 600 m in diameter. Hence, the crater has been erosionally widened by ~150 m and infilled by ~50 m of sediments. Eolian processes are responsible for most crater modification, but lesser mass wasting or gully activity contributions cannot be ruled out. Erosion by prevailing winds is most significant along the exposed rim and upper walls and accounts for ~50 m widening across a WNW–ESE diameter. The volume of material eroded from the crater walls and rim is ~20% less than the volume of sediments partially filling the crater, indicating eolian infilling from sources outside the crater over time. The annulus formed when ~1 m deflation of the ejecta created a lag of more resistant hematite spherules that trapped <10–20 cm of darker, regional basaltic sands. Greater relief along the rim enabled meters of erosion. Comparison between Victoria and regional craters leads to definition of a crater degradation sequence dominated by eolian erosion and infilling over time.

Citation: Grant, J. A., S. A. Wilson, B. A. Cohen, M. P. Golombek, P. E. Geissler, R. J. Sullivan, R. L. Kirk, and T. J. Parker (2008), Degradation of Victoria crater, Mars, *J. Geophys. Res.*, *113*, E11010, doi:10.1029/2008JE003155.

1. Introduction

[2] The ~750 m diameter Victoria crater in Meridiani Planum, Mars (1.9483°S, 354.4742°E, Figure 1), is the largest crater explored by either the Opportunity or Spirit Mars Exploration Rover since their landings in January 2004 [e.g., *Squyres et al.*, 2004; *Golombek et al.*, 2006a; *Grant et al.*, 2006]. Like many craters explored by Opportunity to date, Victoria is a relatively simple, bowl-shaped structure that presents considerable evidence for significant degradation: (1) it displays a low, serrated, raised rim characterized by alternating alcoves and promontories, hereafter referred to as "bays" and "capes," respectively; (2) it is surrounded by a low-relief annulus (Figure 2); and (3) the crater floor is partially covered by dunes (Figure 1). We define the raised rim as the extent (vertically and laterally) of the relief bounding the crater, consisting of contributions from both structurally uplifted rocks and ejecta [*Melosh*, 1989]. Although surfaces beyond the limit of uplifted rocks are mantled by ejecta and rise above the level of the preimpact surface, they are not considered here to be a part of the rim. The annulus is defined as the region extending from the edge of the raised rim to the exposed preimpact bedrock surface beyond and is characterized by extremely low-relief surfaces consisting mostly of dark-toned basaltic sand and a widespread cover of large hematite concretions [*Soderblom et al.*, 2004; *Weitz et al.*, 2006; *Sullivan et al.*, 2007]. Note that the names of all places and features at Victoria crater were assigned for planning and operations purposes and are not recognized by the International Astronomical Union.

[3] The degraded form of impact craters on the Earth and Mars reflects the cumulative influence of geomorphic processes, including the potential role of water, that have contributed to their modification. Therefore, identifying diagnostic signatures associated with specific geomorphic processes and comparing the expected scale of various parameters for a pristine crater (e.g., raised rim height and depth-to-diameter ratio [*Melosh*, 1989; *Garvin et al.*, 2000, 2003]) to what is observed can constrain the amount and relative importance of the processes contributing to the degradation of the crater. Techniques based on this approach constrain the degradation history of simple, unglaciated terrestrial craters, including contributions by various processes [*Grant and Schultz*, 1993a; *Grant et al.*, 1997; *Grant*, 1999], and have successfully been applied to craters on Mars using orbital data [*Grant and Schultz*, 1993b] and data

[1]Center for Earth and Planetary Studies, National Air and Space Museum, Smithsonian Institution, Washington, D. C., USA.
[2]Marshall Space Flight Center, Huntsville, Alabama, USA.
[3]Jet Propulsion Laboratory, California Institute of Technology, Pasadena, California, USA.
[4]U.S. Geological Survey, Flagstaff, Arizona, USA.
[5]Department of Astronomy, Cornell University, Ithaca, New York, USA.

0148-0227/08/2008JE003155$09.00

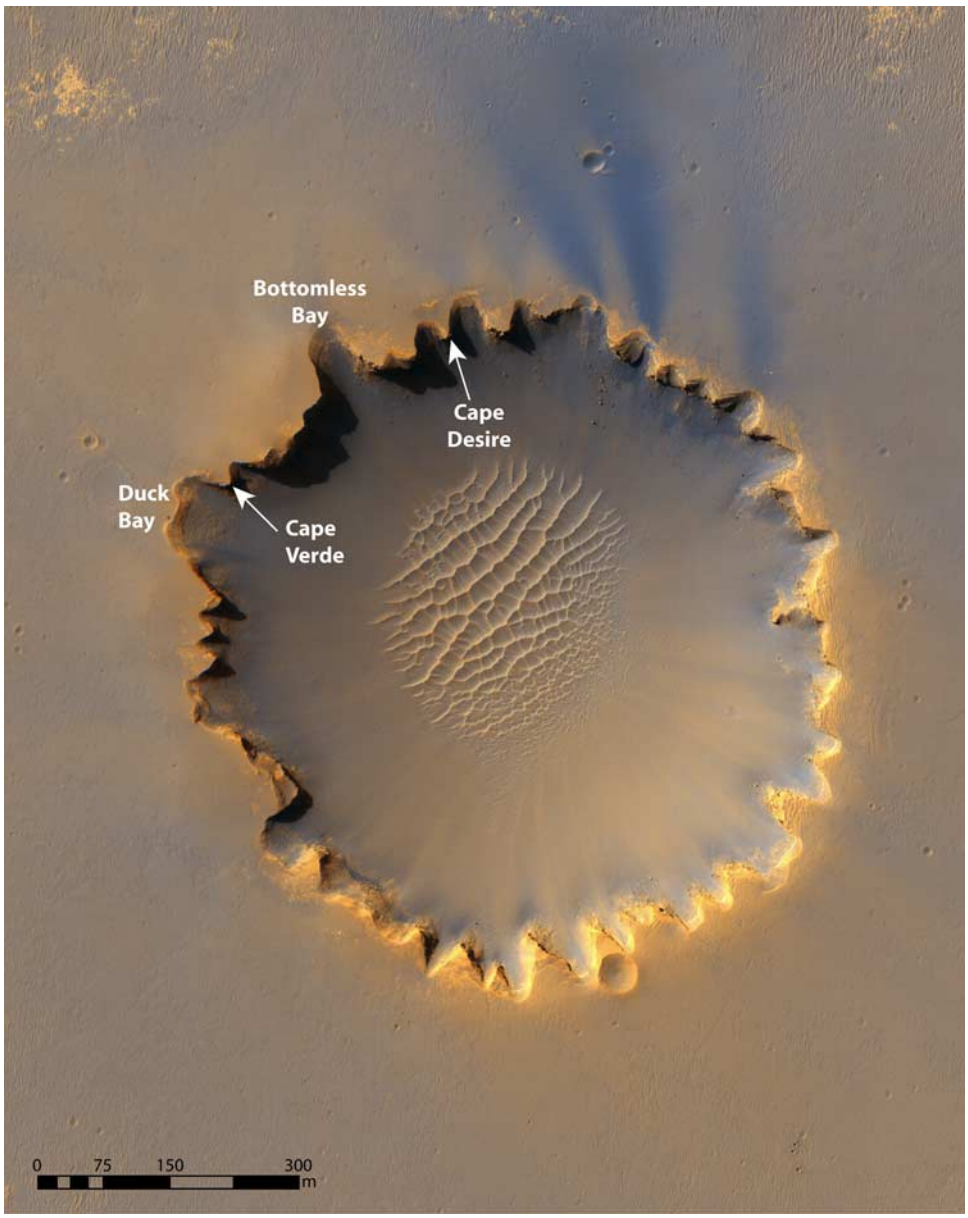

Figure 1. Color HiRISE image (subframe of TRA_000873_1780 IRB) of Victoria crater showing the serrated rim plan and locations of Duck Bay, Cape Verde, Bottomless Bay, and Cape Desire (shown in Figure 4 and discussed in text). Note the dark streaks extending to the NNW from the northern bays or rim alcoves. The Opportunity rover approached the crater along the western edge at Duck Bay before traversing along the northern edge of the crater and eventually returning to Duck Bay and entering the crater. North is to the top of the image.

returned by the Mars Exploration Rovers [*Grant et al.*, 2006; *Golombek et al.*, 2006a, 2006b].

[4] At Victoria crater, in situ observations by the Opportunity rover in tandem with measurements from a digital elevation model (DEM) produced using a pair of stereo images (26 cm/pixel scale) from the High Resolution Imaging Science Experiment (HiRISE) [*McEwen et al.*, 2007] enable a similar approach to evaluating degradation state. These observations and measurements at Victoria were used to quantify current crater parameters including depth-to-diameter ratio, raised rim height and width, ejecta thickness and likely extent, and the slope of the crater walls. Measurements were compared to values predicted for pristine craters of varying sizes to identify whether the crater is primary or secondary and to evaluate how much degradation the crater has experienced. Morphologic signatures created during crater degradation were identified and used to interpret the responsible processes. Finally, results are compared to observations of craters in the vicinity of Victoria to define a generalized crater degradation sequence.

2. Predicting Pristine Morphology for Simple Craters

[5] The pristine morphology of impact craters and their associated ejecta deposits is well understood [e.g., *Quaide*

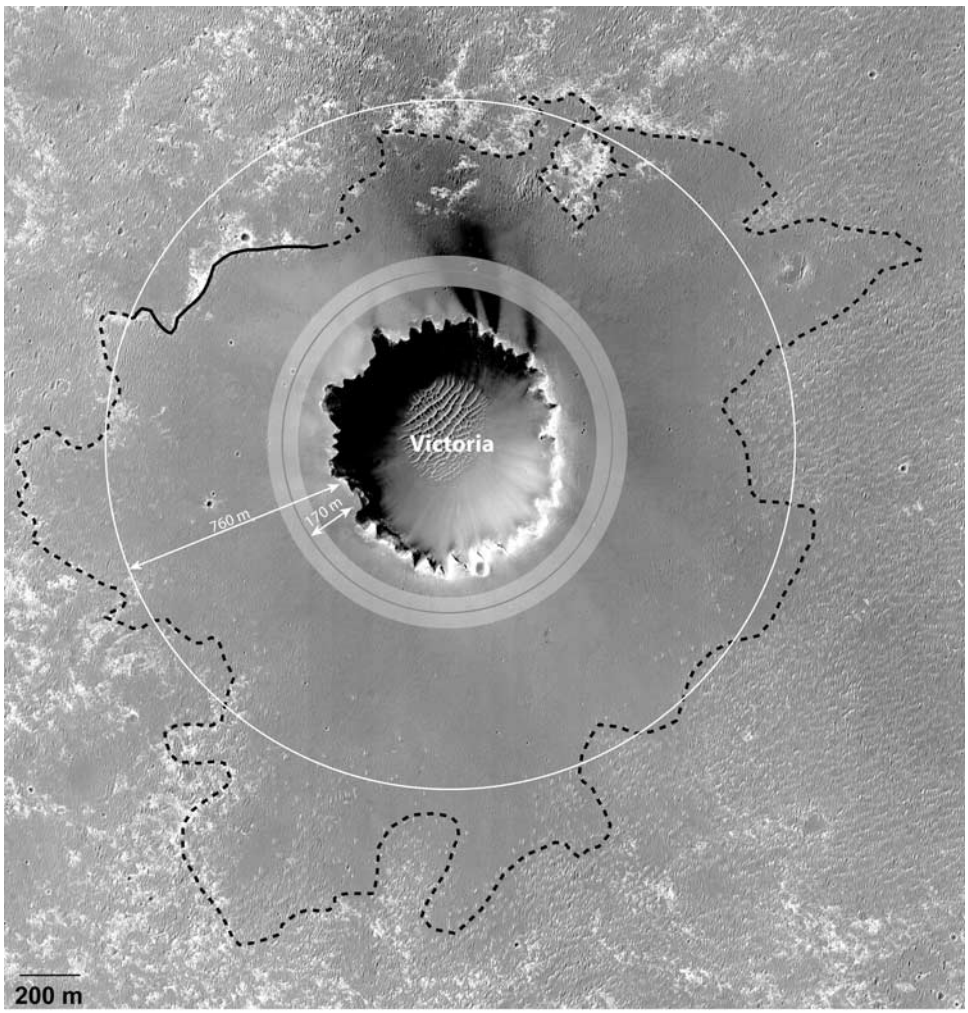

Figure 2. HiRISE image (subframe of PSP_001414_1780 red channel) of Victoria crater and surrounding annulus (outlined in black and dashed where approximated). The annulus presents a very low relief surface (Figure 10) that is largely free of blocks and outcrops and is dark toned relative to surrounding surfaces. The annulus begins beyond the raised rim, and its distal edge is roughly centered on the crater, averaging 590 m beyond the average extent of the raised rim (gray line; the width of the raised rim ranges from 120 to 220 m beyond the rim crest as shown by the shaded white band), or 760 m from the current rim crest (white line). The position of the annulus relative to the crater suggests that it is not a regional geologic or geomorphic contact and that its origin is related to the crater. North is to the top of the image.

and Oberbeck, 1968; *Gault et al.*, 1968; *Gault*, 1970; *McGetchin et al.*, 1973; *Moore et al.*, 1974; *Shoemaker and Kieffer*, 1974; *Pike*, 1977a, 1977b; *Roddy*, 1978; *Schultz and Gault*, 1979; *Melosh*, 1989; *Schultz*, 1992]. Although aspects of crater morphology vary from crater to crater [e.g., *Garvin et al.*, 2000], and the origin of some attributes remains controversial (e.g., the origin of rampart ejecta facies around craters on Mars [*Barlow*, 2005]), many morphometric and morphological characteristics can be interpreted or modeled with reasonable confidence [*Melosh*, 1989]. Nevertheless, impact target effects, impact angle, and other factors can influence aspects of crater morphology and individual components of craters (e.g., the height of the raised rim or ejecta thickness) are best described by a range of predicted values [*Melosh*, 1989].

[6] Pristine primary craters less than several kilometers in diameter are characterized by a simple, bowl-like shape and a well-defined raised rim [e.g., *Melosh*, 1989]. Relationships between the dimensions of the late stage transient cavity and those of the final crater as well as the characteristic raised rim height with respect to crater diameter can be predicted [*McGetchin et al.*, 1973; *Melosh*, 1989; *Garvin et al.*, 2000, 2003]. A model described by *Melosh* [1989] indicates that the transient crater diameter D_t and depth H_t for impacts into solid materials can be related to the final diameter D, depth d, and rim height h_r by

$$D_t = 0.84D, \tag{1}$$

$$H_t/D_t = 1/2.7, \tag{2}$$

$$h_r = 0.035D^{1.014}. \tag{3}$$

Table 1. Comparison of Morphometry of Victoria Crater and a Pristine Crater With a Diameter of 750 m

Crater Parameter	Observed Parameters	Pristine Parameters
Diameter (m)	750	750
Transient crater diameter (m)	uncertain	630
Depth (m)	75	150
d/*D* ratio	0.1	0.2
Current or initial extent of annulus or ejecta (m)	760[a]	750[b]
Total pristine rim height at crest (m)	~5[c]	29 (19–42)[d]
Uplift observed and predicted at rim (m)	~1–2[e]	~10–21[f]
Thickness of ejecta at crater rim (m)	~3.0[g]	~6–20[h]
Width of raised rim (m)	~120–220	~110–260

[a]Average of eight transects that range between 470 and 1100 m.
[b]Assuming that ejecta extends ~1*D* beyond the original rim [*Wilhelms*, 1987; *Grant and Schultz*, 1993b].
[c]Rim height averages 5 m (ranges between 4 and 6 m) based on profiles from north and south of Victoria with regional slope removed.
[d]Value from equation (3) [e.g., *Pike*, 1977a]. Factor of 1.5× range in parentheses.
[e]Inferred from the difference between measured rim height and measured thickness of ejecta at the rim.
[f]Range assuming that uplift comprises approximately one half of the total rim height at the crest [*Shoemaker and Kieffer*, 1974; *Melosh*, 1989].
[g]On the basis of measurements from the Opportunity rover images and HiRISE DEM which yield similar results.
[h]Range assuming that ejecta comprises approximately one half of the total rim height at the crest [see *Shoemaker and Kieffer*, 1974; *Melosh*, 1989; *McGetchin et al.*, 1973, equation (4)].

Rim height h_r is partly due to structural uplift of near-rim target rocks and partly due to emplacement of ejecta deposits from the crater [*Melosh*, 1989]. Measurements of simple lunar and terrestrial craters [e.g., *Pike*, 1977a] all display rims whose heights are within a factor of about 1.5 of what is predicted by equation (3) [*Pike*, 1977a; *Melosh*, 1989] and indicate that the equation is appropriate for use at Victoria on Mars. Rim uplift typically accounts for approximately 50% of the rim height at the rim [*Shoemaker and Kieffer*, 1974; *Melosh*, 1989], but measurements around simple terrestrial impact and nuclear explosion craters indicate that uplift contributions decay to zero at a range of 1.3–1.7 crater radii [*Roddy et al.*, 1975; *Melosh*, 1989]. Data from terrestrial craters, explosion craters, and smaller laboratory craters can be used to gain estimates of the thickness of the near-rim ejecta deposit E_t in meters [*McGetchin et al.*, 1973]. E_t can be related to the transient crater radius R_t and radial distance r from the crater rim, where $r > R_t$ [*McGetchin et al.*, 1973]:

$$E_t = 0.14 R_t^{0.74} (r/R_t)^{-3.0}. \quad (4)$$

Values derived using equation (4) can vary from measurements of ejecta thickness made using images of craters. Such variability is due to radial differences in ejecta thickness around a crater, incorporation of target rocks into the ejecta deposit, and other factors [*Melosh*, 1989], thereby suggesting that values derived using equation (4) should be viewed as approximations. Ejecta deposits on the Moon [*Moore et al.*, 1974; *Wilhelms*, 1987; *Melosh*, 1989] and Earth [*Grant and Schultz*, 1993a] typically extend up to a crater diameter beyond the rim, thereby implying that it is reasonable to expect a similar extent on Mars.

[7] For simple craters excavated by primary hypervelocity impactors arriving from space (traveling at speeds greater than a few kilometers per second), the final pristine depth-to-diameter ratio, *d*/*D*, is typically ~0.2 [*Pike*, 1977b; *Pike and Wilhelms*, 1978] but may approach ~0.3 to ~0.5 for some craters on Mars that are only ~10 to ~100 m in diameter [*Garvin et al.*, 2003]. For secondary craters on Mars, which form as slower-moving material ejected during the primary impact event reimpacts the surface some distance away, rims and planform can be somewhat more irregular than for primary craters, and *d*/*D* is typically ~0.10 [*Pike and Wilhelms*, 1978; *Pike*, 1980; *Melosh*, 1989; *Hurst et al.*, 2004; *McEwen et al.*, 2005]. Although less predictable, impacts into layered targets can produce benches on crater walls, influencing expected pristine crater morphology [*Quaide and Oberbeck*, 1968].

[8] Insight into the amount of degradation and the processes responsible for modifying Victoria's original form can be gleaned by studying its preserved morphology and comparing the current form to the form expected for pristine craters of varying sizes. Measurements from Pancam images taken by Opportunity and the HiRISE DEM yield similar results and provide a consistent characterization of Victoria's current form.

3. Victoria's Present Dimensions

[9] Victoria crater is approximately 750 m in diameter and 75 m deep, yielding a depth-to-diameter ratio, *d*/*D*, of 0.1 (Table 1), which is less than expected for a pristine primary crater [*Pike*, 1977b]. The diameter of Victoria is ~50 m wider in the WNW to ESE direction, which is aligned with some of the most prominent bays along the rim and is generally consistent with the direction of current, prevailing winds that have influenced ripples preserved on the plains outside of Victoria and active nearby wind streaks [*Sullivan et al.*, 2005; *Jerolmack et al.*, 2006] (Figure 3). The crater floor is mantled by dunes and drift that partially fill the crater.

[10] Measurements from rover images and the HiRISE DEM, normalized for regional slopes, constrain rim relief and detail contributions from ejecta and uplift. Removing the effects of regional topography was most useful on the south and southeast sides of the crater where decreasing elevation away from the rim made it difficult to extract the relief and the extent of the raised rim. Confidence in rim heights and width is highest on the north side of the crater where rim relief decreases in a direction opposite to the regional gradient and measurements are directly derived from rover-based images and the HiRISE DEM. Measurements reveal that the rim rises 4–6 m (averages ~5 m) above the surrounding annulus and extends approximately 120–220 m beyond the rim crest (Table 1). Rover images show that rim relief at the crest consists of ~1–2 m of uplifted rocks that are overlain by an average of ~3 m of ejecta (Figure 4). The annulus surrounding Victoria, discussed further in section 7, extends an average of 590 m beyond the raised rim or 760 m from the rim crest (Figure 2 and Table 1).

4. Predicting Victoria Crater's Original Dimensions

[11] If Victoria's original diameter was 750 m and the crater resulted from a primary impact event and retained a

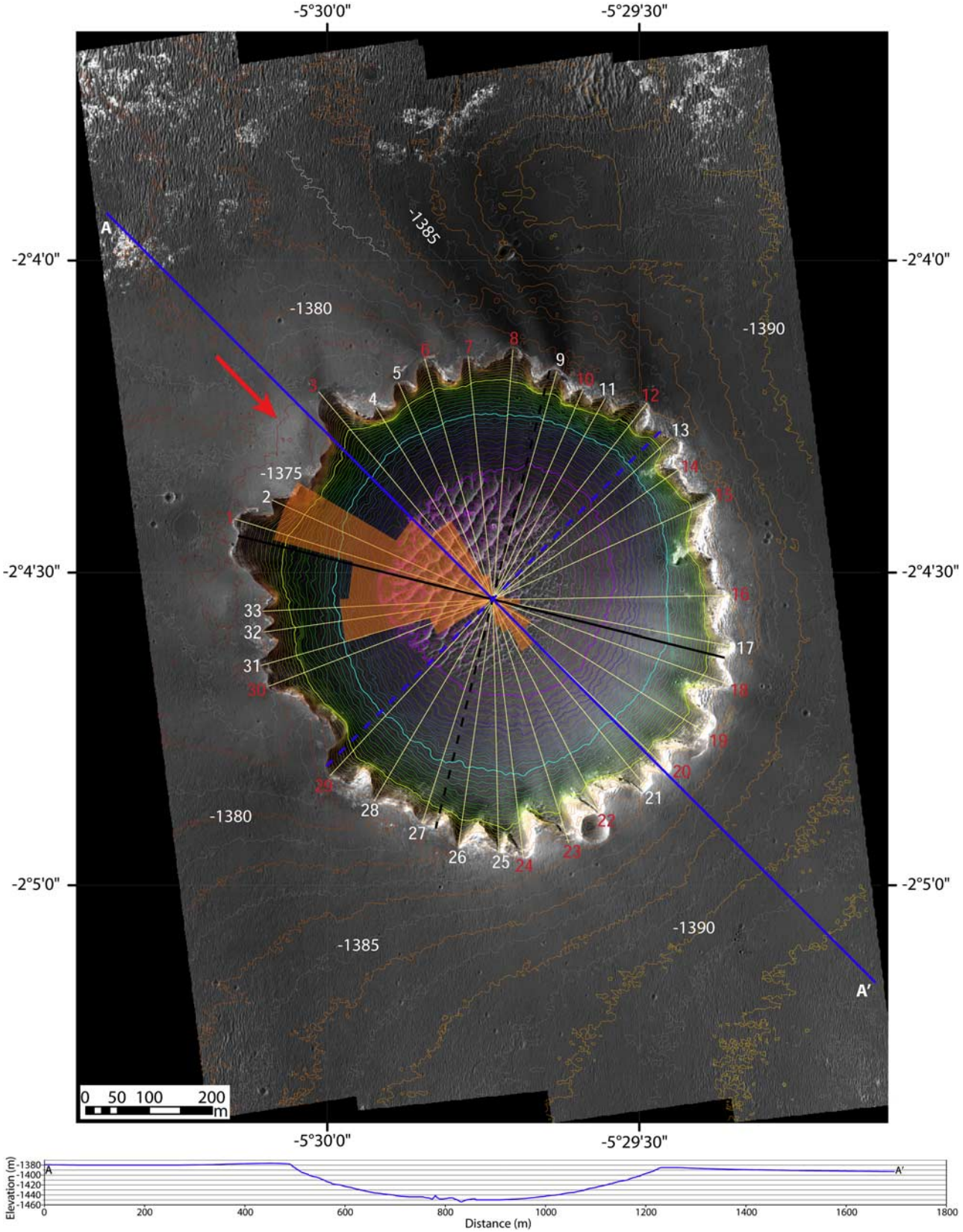
-5°30'0"
-5°29'30"
-2°4'0"
-2°4'30"
-2°5'0"
A
A'
-1385
-1380
-1390
-1375
1
2
3
4
5
6
7
8
9
10
11
12
13
14
15
16
17
18
19
20
21
22
23
24
25
26
27
28
29
30
31
32
33
0 50 100 200
m
Elevation (m)
-1380
-1400
-1420
-1440
-1460
0
200
400
600
800
1000
1200
1400
1600
1800
Distance (m)

Figure 3

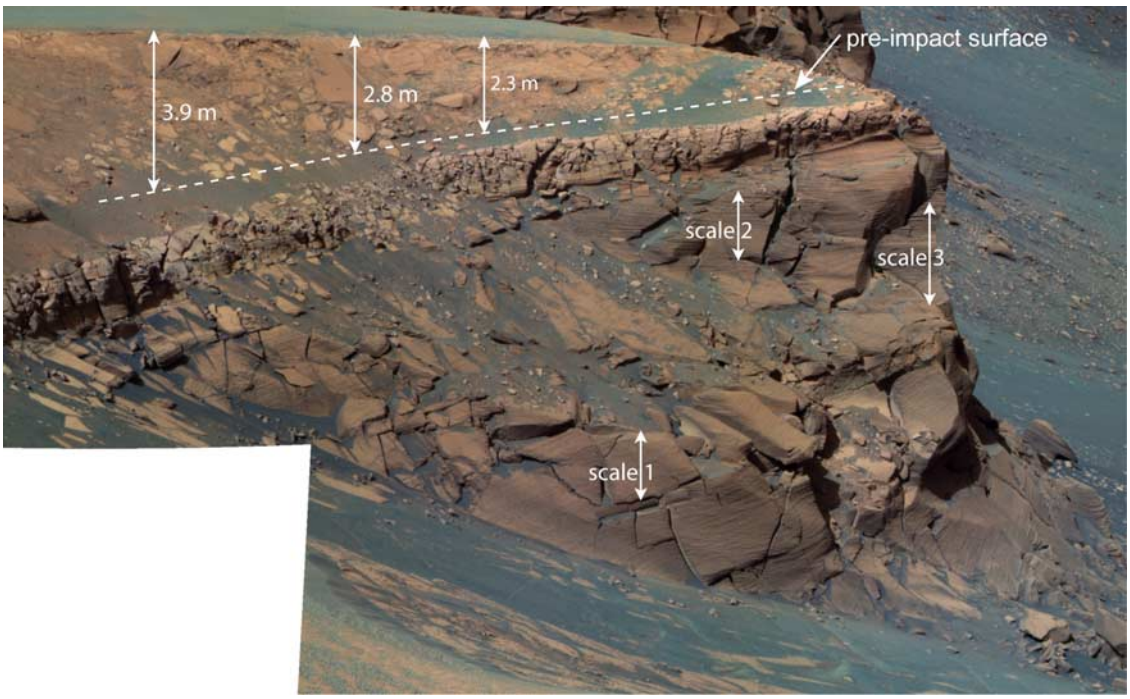

Figure 4. Rover-based mosaic of the west face of Cape Desire on the north rim of Victoria crater (see Figure 1 for context). Vertical lines provide examples of where the thickness of the ejecta around the rim of the crater was measured using Pancam images. The dashed line shows the boundary of ejecta (above) and preimpact surface (below) that was identified on the basis of comparison between stratigraphy exposed on the upper wall and beyond the annulus and was confirmed by the upward transition from fractured but largely in-place rocks to an overlying jumbled and blocky deposit possessing mixed lithologies. On the basis of in situ study at Duck Bay, the prominent light-toned marker bed occurs ~0.5 m below the preimpact surface and is visible in all rover and HiRISE images of the crater. Tracing this light-toned bed around the crater enables the base of the ejecta to be estimated with confidence. Ejecta thickness was derived from multiple measurements (average of five) using Science Activity Planning tools on vertical or near-vertical faces. In this image, scale 1 is 1.1 m (~27.6 m from the rover), scale 2 is 1.9 m (35 m from the rover), and scale 3 is 2.75 m (37.7 m from the rover). Note the scoured appearance of the base of the cape and the draping of darker, regionally occurring basaltic sands across the cape and intervening bay that indicate sediment transport into and out of Victoria crater. False color Pancam mosaic created using sequence p2350 and L257 filters (RGB = 753, 535, and 432 nm) taken on Martian solar day (sol) 1060 of Opportunity's mission.

pristine form, then a depth of 150 m and a d/D ratio of 0.2 are expected [*Pike*, 1977b; *Pike and Wilhelms*, 1978; *Melosh*, 1989]. The predicted rim height of such a crater from equation (3) is 29 m, but including a factor of 1.5× uncertainty suggests a possible range of 19–42 m. Rim width would be between 110 and 260 m, assuming that it extends to $1.3R$–$1.7R$. The pristine rim should be composed of up to ~14 m of ejecta overlying ~15 m of uplifted rocks

Figure 3. HiRISE image PSP_001612_1780 red channel overlain by 1 m contours derived from a stereo pair (PSP_001414_1780 and PSP_001612_1780, 26 cm/pixel resolution) of Victoria crater used to create a DEM (U.S. Geological Survey, University of Arizona, NASA, and Jet Propulsion Laboratory). Heavy green, cyan, and purple contours within Victoria highlight 20 m intervals and correspond to −1400, −1420, and −1440 m, respectively. Locations of profiles down bays are in yellow and shown in Figure 6. Red and white numbers at the top of the profiles indicate whether the difference in slope between the head of the bay (to best fit contour at the base of the capes at −1402 m) and the entire profile (to −1434 m, edge of dune field) is 0.5°–4.9° or 5.0°–14.2°. The orientations of rock tails around the crater suggest that winds at 284° ± 28° and 135° ± 25° [*Sullivan et al.*, 2005] predominated, as shown by the superposed rose diagram (modified from *Sullivan et al.* [2005]). Red arrow indicates the present wind direction from the northwest based on the orientation of ripples on the floor of Eagle crater and the location of the bright wind streak outside of Eagle crater, representing a ~40° clockwise shift from previous wind directions interpreted from the orientation of older plains ripples [*Sullivan et al.*, 2005]. The diameter of the crater aligned with the mostly west to northwest winds (solid black and blue lines) is approximately 50 m larger than the diameter measured 90° away (dashed black and blue lines). Profile across the crater and annulus was completed along the solid blue line from A to A′ (NW–SE) and is not vertically exaggerated.

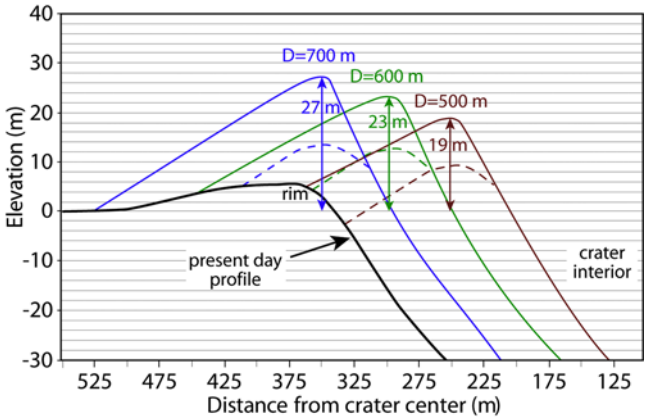

Figure 5. Comparison between the observed profile across the rim of Victoria crater (heavy black line) and relief and position of idealized rim forms associated with pristine craters initially 500 (red line), 600 (green line), and 700 m (blue line) in diameter. Dashed lines represent the approximate contributions to rim relief from ejecta (above dashed lines) and uplift (below dashed lines) for each case. Idealized rims shown drop to the level of the surrounding plains at a distance of 1.5*R*, but may range between 1.3*R* and 1.7*R* [*Melosh*, 1989]. After erosion to the current diameter, the crater initially 600 m across yields a rim composed of both ejecta and uplifted rocks as is observed. A crater initially 500 m across eroded to the current diameter likely results in destruction of the raised rim, whereas a crater initially 700 m across creates a raised rim of only uplifted rocks if eroded to the current profile.

at the crest (Table 1), assuming that uplift and ejecta make approximately equal contributions [*Shoemaker and Kieffer*, 1974; *Melosh*, 1989]. Estimated ejecta thickness at the rim from equation (4), however, is ~6 m, suggesting a factor of approximately 2× uncertainty in predicted ejecta contributions to rim relief. Regardless, the portion of the rim relief attributable to uplift at the crest would exceed the total rim relief presently observed at Victoria. Finally, the ejecta surrounding the crater would consist of deposits reaching about one crater diameter or ~750 m from the rim crest [*Wilhelms*, 1987; *Grant and Schultz*, 1993a].

[12] The observed rim width at Victoria is within the range predicted for a pristine crater close to its present size. Similarly, the expected extent of ejecta is comparable to the observed extent of Victoria's annulus and may suggest that it relates to the crater's ejecta deposit [*Sullivan et al.*, 2007; *Grant et al.*, 2008]. By contrast, the observed values for the *D*/*d* ratio, rim relief, and estimated contributions by both ejecta and uplift contradict the predicted appearance of a pristine 750 m diameter primary crater and point to considerable degradation. Moreover, the serrated rim plan and the presence of dunes on the crater floor indicate that some modification has occurred and that Victoria is not a pristine secondary impact crater, despite the *D*/*d* ratio of 0.1. Hence, Victoria is neither a pristine primary nor a secondary crater but is the degraded form of an originally smaller and/or likely deeper primary impact crater.

[13] The amount of modification at Victoria crater can be approximated by evaluating the expected depth, rim height, rim width, and extent of ejecta for a range of pristine primary crater sizes and comparing derived values to those measured at Victoria (Figure 5). To get a sense of the range and sensitivity of these parameters to changing crater size, focus was placed on modeling pristine primary craters between 500 and 700 m in diameter (Table 2) for comparison to what is observed and predicted at Victoria (assuming a 750 m diameter crater with no erosion) (Table 1).

[14] A pristine 500 m diameter primary crater should have a depth of ~100 m and a 19 m high (ranges between 13 and 28 m) and approximately 75–175 m wide rim (Table 2). If enlarged to the present 750 m diameter, however, the raised rim would be completely removed or would persist only as a very low, less than ~50 m wide, ribbon around the

Table 2. Morphologic Characteristics Calculated for Pristine Craters of Varying Diameters[a]

Crater Parameter	Scenario 1 (*D* = 500 m)	Scenario 2 (*D* = 550 m)	Scenario 3 (*D* = 600 m)	Scenario 4 (*D* = 650 m)	Scenario 5 (*D* = 700 m)
Transient crater diameter (m)	420	462	504	546	588
Depth (m)	100	110	120	130	140
d/*D* ratio	0.2	0.2	0.2	0.2	0.2
d/*D* for 750 m diameter crater	0.13	0.15	0.16	0.17	0.19
Initial extent of ejecta[b] (m)	500	550	600	650	700
Extent of ejecta from rim if enlarged to 750 m diameter (m)	375	450	525	600	675
Total pristine rim height at crest[c] (m)	19 (13–28)	21 (14–32)	23 (15–35)	25 (17–38)	27 (18–40)
Rim uplift at current rim[d] (m)	0 (0–4)	3 (0–8)	~6 (1–11)	~9 (4–15)	~12 (7–18)
Thickness of ejecta at current rim[e] (m)	>1.3	>1.8	>2.5	>3.5	>5
Width of raised rim (m)	~0–50	~0–90	~15–135	~50–175	~80–220

[a]Victoria crater is currently ~750 m in diameter and ~75 m deep, yielding a *d*/*D* ratio of 0.1. Assuming that Victoria is a pristine and a primary crater, a *d*/*D* ratio of ~0.2 is expected [*Melosh*, 1989]. Obvious evidence for infilling (e.g., dunes) and enlargement (e.g., serrated rim plan) suggest that the crater is degraded and was initially deeper and smaller in diameter.

[b]Assuming that ejecta extends ~1*D* beyond the original rim [*Wilhelms*, 1987; *Grant and Schultz*, 1993b].

[c]Value from equation (3) [e.g., *Pike*, 1977a]. Factor of 1.5× range in parentheses.

[d]Assumes that uplift and ejecta each comprises approximately one half of the total rim height at the initial crest [*Shoemaker and Kieffer*, 1974; *Melosh*, 1989]. These values are compared to expected values at *R* = 375 m if uplift decays to zero at a range of 1.5*R*. Range is for minimum and maximum estimates of rim height where uplift decays to zero at 1.3*R* and 1.7*R*.

[e]Calculated using equation (4) and data from *Moore et al.* [1974] (reproduced by *Melosh* [1989]). Actual value may be ~2× larger on the basis of comparison with ejecta thickness estimated at the original rim crest as a component total rim relief (see footnote c above).

crater (assuming no vertical erosional lowering of the surface, see Table 2). In fact, the only way that a 500 m crater could produce a rim possessing 1–2 m of uplift at the present diameter involves the unlikely case where the original rim height was the maximum 28 m and the original rim extent was the maximum 1.7*R*. At a diameter of 750 m, ~1.3 m ejecta are predicted from equation (4), but a thicker section could be present if ejecta contributions comprised ~50% of initial rim relief [*Shoemaker and Kieffer*, 1974; *Melosh*, 1989]. Nevertheless, the height and width of the raised rim at Victoria appear difficult to reconcile with enlargement of a crater initially 500 m across. Further, the observed crater depth is less than predicted for a 500 m diameter crater and the ejecta would have had to reach 1.75*D* beyond the original rim to account for the observed annulus. Collectively, these characteristics require a crater originally larger than 500 m in diameter to be consistent with the observed parameters at Victoria (Figure 5).

[15] A 700 m diameter pristine primary crater would be ~140 m deep, and equation (3) yields a 27 m high rim (range of 18–40 m) that would be 105–245 m wide (Table 2). If enlarged to 750 m across, the crater should retain at least 12 m relief (more than 7 m uplift and 5 m ejecta from equation (4), see Table 2), forming a rim extending 80–220 m from the crest (assuming no vertical erosion). To achieve the observed ~5 m of rim relief at Victoria by enlarging a 700 m diameter crater, all ejecta would have to be eroded away, leaving only uplifted rocks to form the rim. Because rover images show that Victoria's rim is a combination of uplifted rocks and ejecta (Figure 4), a crater initially 700 m across is too large to account for observed rim characteristics and other crater morphology, suggesting that the original Victoria crater was between 500 and 700 m in diameter (Figure 5).

[16] If Victoria was initially 650 m in diameter and 130 m deep, equation (3) predicts a 25 m high pristine rim (range of 17–38 m) that would be 100–225 m wide at the original crest. If enlarged to 750 m, the raised rim would be at least 7–8 m high (assuming no vertical erosion) and consist of at least 4 m of uplift capped by a minimum of 3.5 m of ejecta (from equation (4), see Table 2). Ejecta deposits would likely reach ~600 m beyond the present rim.

[17] A 600 m diameter crater would be 120 m deep, and equation (3) predicts a 23 m high rim (range of 15–35 m) that would be 90–215 m wide. Enlargement to 750 m across (without vertical erosion) yields a rim 30–150 m wide and at least 3–4 m high. The rim would consist of at least 1 m of uplifted rocks beneath a minimum of 2.5 m ejecta (from equation (4), see Table 2). Ejecta would reach ~525 m beyond the present rim.

[18] Finally, a 550 m diameter crater would be 110 m deep, and equation (3) indicates an encompassing rim 21 m high (range of 14–32 m) and 83–193 m wide. If widened to 750 m in diameter (without vertical erosion), a raised rim including several meters of uplifted rocks may persist (for the unlikely case where the original rim height and width are both maximized) but would be no more than 90 m wide. Ejecta would be at least 1.8 m thick at the present rim crest (from equation (4)) and would either cap the uplifted rocks if the raised rim persists or would contribute to the annulus if it does not. Ejecta would be expected to extend ~450 m from the present rim.

[19] A primary crater on the order of 600 m across that has widened to the present diameter of Victoria would likely preserve a remnant rim consisting of both ejecta and uplifted target rocks, which is generally consistent with observations. In this scenario, vertical erosion at the current rim would have removed ~3–6 m of material, leaving the 1–2 m uplifted rocks and ~3 m of ejecta observed (Table 2). The predicted width of the remnant raised rim associated with a crater initially 600 m across that is enlarged to Victoria's current diameter is less than, but approaching the range of, what is observed. The extent of ejecta around such a crater is also less than the observed extent of the annulus in most directions (Figure 2). Finally, the current crater depth is less than the 110–130 m predicted for all pristine craters between 550 and 650 m across, but this is likely due to infilling by debris that includes material eroded from the backwasting walls and sand blown in to create the dunes within the crater.

[20] Although craters initially larger than 600 m across may produce a better match to the rim width and extent of the annulus, they cannot preserve a raised rim consisting of the mix of uplift and ejecta that is observed. By contrast, craters initially smaller than 600 m might preserve a rim composed of both uplifted rocks and ejecta if enlarged to 750 m, but those rims would be unrealistically narrow, and the extent of any remaining ejecta would be a poor match to the extent of the annulus. Most likely, differences between values predicted for an enlarged 600 m crater versus what is observed at Victoria crater are due to variables such as target strength differences, impact angle effects, etc.

[21] A primary crater originally 600 m in diameter that is eroded and widened to the current diameter of Victoria provides the best fit to observed crater parameters and dimensions (Figure 5). This erosion would impart the planed-off appearance of exposed ejecta blocks and the overall low local relief along the rim (Figures 1 and 4). If correct, Victoria has been widened by about 150 m and has been subjected to ~50 m of infilling (partly accommodated by eolian deposits).

[22] Simple calculations enable comparison of the contributions to crater fill from erosion of the wall and rim relative to the volume of fill within the crater. To do this, the rim and wall are assumed to have downwasted and backwasted 18 and 75 m, respectively, to the current level of the rim. To account for additional material eroded from the wall below the rim, the 75 m average backwasting at the rim was assumed to taper to about 40 m at the current level of the crater fill and then taper completely at about 30 m below the current level of the crater fill. Collectively, these contributions from rim and wall erosion comprise approximately 6.2×10^6 m^3 of material. Volume changes related to density differences between the wall rock and the eroded sediment were not considered because the exposed walls are dominated by weakly cemented and highly fractured eolian sandstones that should be roughly comparable in density to the derived sediments. The volume of the crater fill was calculated assuming a radius of 280 m at the top of the fill that tapered to a radius of 220 m at the crater floor. On the basis of assumed initial dimensions for a crater originally 600 m across, the fill is ~50 m deep near the center of the crater but is observed to rise an additional 28 m at the base of the walls (Figure 3). The volume of crater fill is 7.7×10^6 m^3

using these dimensions, which is ~20% more than the volume predicted to have eroded from the walls and rim. This difference is likely due to infilling contributions from a variety of regional sources [*Geissler et al.*, 2008] and is consistent with the presence of dark-toned drift in the crater [*Sullivan et al.*, 2007; *Geissler et al.*, 2008]. Moreover, the friable nature of the sulfate rocks [*Okubo*, 2007] makes them susceptible to erosion that leaves little behind except resistant hematite concretions [*Yen et al.*, 2005] and suggests that crater infilling from regional sources is even more important than described above. The form of the crater preserves additional evidence for the processes responsible for degradation and is discussed further in sections 5 and 6.

5. Victoria's Present Form

[23] The prominent bays and capes forming Victoria's walls are responsible for the serrated appearance of the rim (Figure 1). Bay centerlines are radial to subradial to the crater center, and bay heads are rounded to subangular in plan view. Bays extend an average of 50 m into the rim and plains surrounding the crater, ranging between 25 and 95 m, and partly accommodate the 150 m widening interpreted in section 4. The two deepest bays, dubbed Duck Bay and Bottomless Bay (Figure 1), extend 95 and 74 m into the rim, respectively. Bay surfaces slope into the crater at an average of 19° (range from 14° to 26°), well below the angle of repose (Figure 6). Slopes down the floors of bays having well-rounded heads are generally more uniform along profile, and bay-to-bay profiles are more similar than slopes along bays with less rounded heads (Figure 6). The slope along many bay floors decreases slightly with distance into the crater and averages 5° steeper on upper sections. Nevertheless, some bays, including Bottomless Bay, become less steep near their heads, and variations in slope are transitional rather than occurring at abrupt inflections (Figure 6). Bay surface roughness is generally low over distances of 1–10 m (Figure 7) with rock surfaces appearing planed off to form ventifacts eroded by sediments blowing into and out of the crater (Figure 8). Lower portions of the bays are often obscured by darker basaltic sands that extend from the deposits on the crater floor, but, where exposed, the upper and middle sections of the bays reveal fractured bedrock surfaces (Figure 7).

[24] The capes separating bays in Victoria vary in appearance, but there are common aspects to their form. For example, all capes expose a sequence of in situ rocks overlain by the ejecta deposit (Figure 4). In at least one instance, however, it is difficult to match up the details of the stratigraphy exposed along a cape with those exposed on the floor of the adjacent bay (e.g., Cape Verde and Duck Bay). Interestingly, there appears to be relatively little difference in the erodibility of the ejecta overlying the capes and the capes themselves. Profiles down the tips of the capes average 41° (range from 31°–48°) but are locally vertical. Most capes are not flanked by significant talus, and their bases often remain exposed and are notched and wind-scoured (Figures 4 and 7). Some talus blocks show an obvious narrowing near their bases, suggesting erosion by saltating sand (e.g., Figure 9), whereas others are partially buried by drift materials.

[25] The crater floor near the base of the walls is largely free of talus (Figure 1) and displays very low relief across distances of tens to hundreds of meters outside of the central dune field (Figure 3). Slopes along the lower walls and floor (outside the dune field) are between 12° and 20°, and contours encircling the floor show very little or no deflection toward the wall or crater center as they cross below bays and capes (Figure 3). Outcrops of bedrock are small and entirely limited to the immediate mouths and tips of bays and capes, respectively (Figures 4 and 7–9). The vast majority of the crater floor is covered by smooth, unconsolidated fines that transition into dunes toward the crater center (Figure 1). Individual dunes are up to 5 m high, and orientation of the dominant crests is inferred to be approximately orthogonal to the present prevailing wind direction [*Sullivan et al.*, 2005] (Figure 3). Sediments on the crater floor are variably toned and produce a pattern of "spokes" of lighter- and darker-toned surfaces that are generally darker overall across the western and northern part of the floor (Figure 1).

6. Predicting Victoria's Degradation Processes

[26] A simple model for degradation of Victoria crater that is consistent with the observed form involves mostly ongoing eolian erosion and deposition associated with sediment transported into, eroded within, and transported out of the crater. While erosion is mostly concentrated along the walls and rim of the crater, net infilling over time by sediments transported from outside the crater and from along the walls is important. Ongoing mass wasting imparts lesser contributions and was likely subordinate to eolian activity for much or all of crater history.

[27] Erosion is fastest where windblown sediment scours exposed and relatively weak bedrock and ejecta. The paucity of talus flanking steep walls, smoothed appearance of bay surfaces, and narrowing near the base of rocks highlight the ease with which rocks at Victoria are eroded (Figures 7–9) and imply that they may be as susceptible to erosion as rocks measured during Opportunity's traverse to Victoria. The strengths of those rocks were found to be comparable to talc and chalk [*Okubo*, 2007] and were easily eroded by the wind [*Soderblom et al.*, 2004; *Weitz et al.*, 2006]. The fact that the ejecta layer appears to have a similar resistance to erosion as the bedrock implies that there is little to no impact melt binding the ejecta deposit and that the ejecta is as susceptible to erosion by the wind as the relatively intact sulfate bedrock.

[28] Evolution of the bays was likely enhanced by wind erosion that exploited structural weaknesses in the wall, such as tear faults [e.g., *Shoemaker and Kieffer*, 1974], that can originate when adjacent rim segments experience differential uplift during crater formation [*Melosh*, 1989]. The presence of these structures may explain the difficulties in correlating stratigraphy between Duck Bay and the adjacent Cape Verde.

[29] Sediment moving into and out of the crater via the bays [e.g., *Geissler et al.*, 2008] creates low sloping, smoothed, and rounded transport surfaces that over time lead to larger and lower sloping bays. In support of this, the two deepest bays (Duck and Bottomless bays) are among the smoothest and lowest sloping and are well aligned with

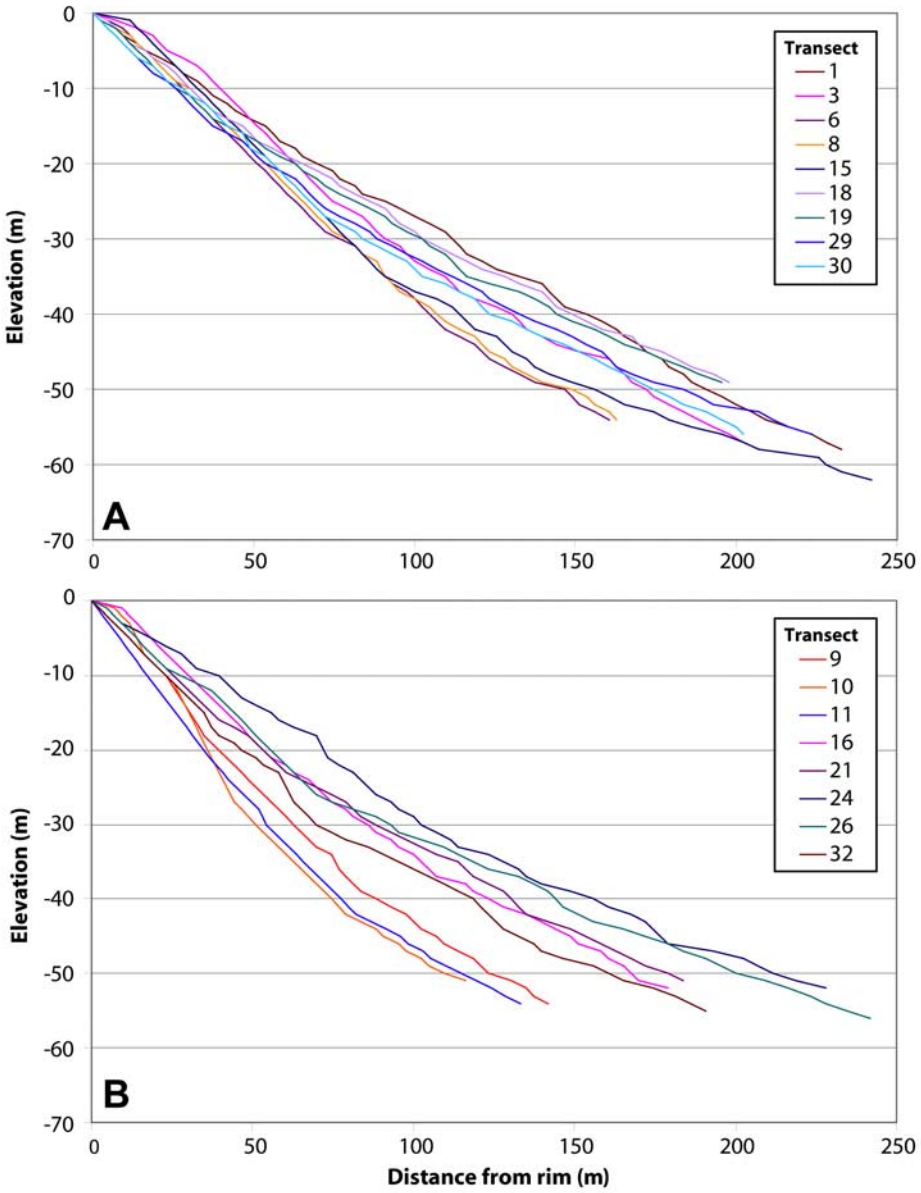

Figure 6. Profiles down Victoria crater bays as derived from 1 m contours from DEM (see Figure 3 for context). Profiles along (a) bays possessing more rounded heads are generally flatter and more uniform than (b) profiles along bays without well-rounded heads. Note that profiles are slightly concave-up but that profiles along some bays (e.g., Bottomless Bay, transect 3) decrease in slope near their heads. Bays with steeper slopes in headward segments (white transect numbers in Figure 3) show gradual transitions in gradient rather than abrupt transitions at well-defined inflections.

the prevailing winds at Meridiani [*Sullivan et al.*, 2005]. Ramps of sediment in the mouths of many bays coupled with the smooth exposures of bedrock and ventifacts (Figure 8) on higher bay surfaces are consistent with this scenario. On a larger scale, wind erosion likely accounts for the 50 m increase in Victoria's diameter occurring in directions consistent with the prevailing winds (Figure 3).

[30] The capes are also dominated by wind erosion, though mass wasting actively contributes to their modification. Wind-induced scour near the base of the capes imparts their often exposed, notched appearance (Figures 4 and 7) and causes oversteepening and collapse. The overall weakness of the talus enables rapid breakdown and/or burial, thereby leaving slopes vulnerable to continued backwasting by both eolian and mass wasting activity. The paucity of talus highlights the dominance of eolian modification in this process and likely reflects a combination of scour by windblown grain impact (Figure 9) and burial of some blocks along the lower walls.

[31] During the initial stages of crater degradation, the more uniformly steep and rubbly walls likely led to a geologically brief interval where mass wasting was more

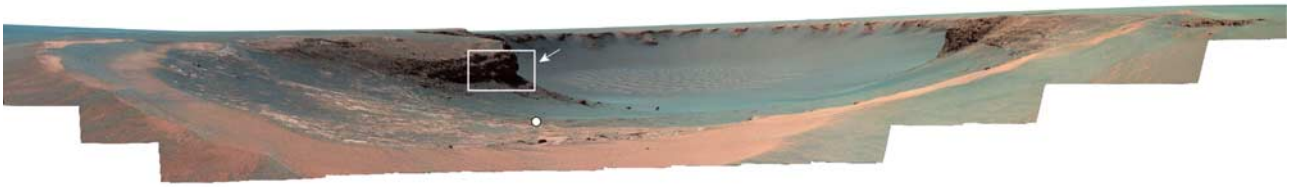

Figure 7. Panoramic mosaic taken by the Opportunity rover looking east into Victoria crater from Duck Bay (see Figure 1 for context). The white dot shows the location of Oppel rock (Figure 8), and the white arrow shows the location of Toledo rock (Figure 9). The box highlights the tip and bounding sides of Cape Verde, which appear notched at the base and are fairly free of flanking talus. Note the smooth expression of the exposed, fractured bedrock on the floor of Duck Bay and ramps of darker basaltic sand on the lower surfaces of this bay and other bays. Mosaic is false color and compiled from Pancam images from sequence p2400 taken on sol 970 using L256 filters (RGB = 753, 535, and 482 nm).

important than at present. Transport of sediment into the crater coupled with rapid breakdown of the exposed walls and talus, however, caused eolian processes to become more important within bays and largely limited additional mass wasting to the capes. Eolian erosion of weaker rocks and/or structure led to evolution of the bays and created surfaces whose profiles enable efficient eolian transport into and out of the crater with only limited accompanying mass wasting. The diminished relief, planed-off appearance of the ejecta blanket, paucity of exposed blocks, and dark wind streaks north of the crater [*Geissler et al.*, 2008] further support efficient eolian modification.

[32] Eroded and redistributed wall materials contribute to crater infilling and/or are transported out of the crater by the wind. Nevertheless, the dark basaltic sands in the crater and wind streaks along the northern rim (Figure 1) are similar to sediments observed on the annulus and plains well beyond Victoria and indicate additional eolian transport into and out of the crater from other sources. Calculation of the volume of material removed from the walls versus that represented by the crater fill indicates that sediments within the crater exceed those eroded from the wall, thereby indicating net infilling over time. Crater fill encroaching into the mouths of bays, examples of partially buried talus (Figure 9), and the flat, featureless expression of the crater floor provide additional evidence for a thickening sequence of fill.

[33] While it is possible that mass wasting or even limited fluvial activity may once have played a more important role in crater degradation and formation of the bays, numerous aspects of their form relative to that expected via mass wasting make this unlikely. Mass wasting produces a broad range of geomorphic forms that are collectively diagnostic of origin [*Varnes*, 1978; *Turner and Schuster*, 1996]. For example, rotational slides or slumps typically possess a concave-up longitudinal profile that becomes steeper and often stepped or terraced near the head scarp. The head or crown of these slides are often curved (in plan view), and there are obvious downslope deposits that persist in the absence of alternate processes capable of their removal. Debris avalanches may be similar in planform but lack a terraced head scarp. Although gravity-assisted flows in Victoria are unlikely on the basis of the outward dip of near-rim rocks, this process cannot be ruled out because of the fragmented appearance of rocks in bay outcrops. Such flows share some of the characteristics of rotational slides but often create an hourglass shape in plan view, with a narrowing near the transition between active excavation and downslope deposition. Like all mass wasting processes, gravity-assisted flows create deposits that should stand in relief relative to adjacent surfaces.

[34] Initiation of the bays as gullies, formed by fluvial or mass wasting activity [e.g., *Grant and Schultz*, 1993b; *Malin and Edgett*, 2000; *McEwen et al.*, 2007; *Pelletier et al.*, 2008], would produce initially smaller forms, incising slopes characterized by steep gradients (e.g., exceeding 21° [*Pelletier et al.*, 2008]) and obvious deposits on lower, less steep portions of the wall. Moreover, alcoves produced by gullies could vary widely in appearance in planform but would likely possess a v-shaped profile in cross section if fluvial activity contributed to their evolution [*Ritter et al.*, 1995]. Few of the coarse-scale characteristics of mass

Figure 8. Oppel rock on the floor of Duck Bay (see Figure 7 for context). Long axis of the rock points in toward the center of the crater (in the direction of the white arrow), and the rock is a ventifact that shows clear evidence for shaping by wind-transported sediment. False color Pancam image using sequence p2594 and L257 filters (RGB = 753, 535, and 432 nm) taken on sol 1342 of Opportunity's mission.

Figure 9. Erosion at the base of the capes produces talus on the lower slopes of the crater wall that is eroded and/or buried. Toledo, the boulder in the center of the image, shows narrowing near its base which we interpret as being due to erosion by wind-transported sediments. Toledo is near the base of Cape St. Vincent (three capes east of Cape Desire) and is approximately 2 m across (see Figure 7 for context). Other blocks nearby appear to protrude from the encroaching fill. False color Pancam image using sequence p2592 and L257 filters (RGB = 753, 535, and 432 nm) taken on sol 1130 of Opportunity's mission.

wasting or gully incision are observed at the Victoria crater bays.

[35] Although many bay heads at Victoria are rounded in plan view (Figure 1), as might be expected for mass wasting forms, others are more angular (e.g., along the southern rim of the crater). Bay floor centerlines are sometimes oriented slightly across slope and show relatively little concavity, and upper sections of some bays actually decrease in slope and are convex near the rim crest (e.g., Bottomless Bay, Figure 6). While bays average $\sim 5^{\circ}$ steeper on upper sections (Figures 3 and 6), some of the deepest bays show the least change in slope along their profiles (e.g., Duck Bay), counter to what is expected for mass wasting scars. Surfaces forming the bays are typically smooth, and obvious terraces or steps are absent. In addition, bay surfaces above the limit of the crater fill expose bedrock, and there is no morphologic or topographic evidence for deposits below any of the bays, as demonstrated by uniformity in contours below both bays and adjacent capes. None of the bays present an hourglass appearance in plan view that might hint at their origin by gravity-assisted flow. Finally, the low gradient along the bays and the u-shaped profiles across the bays coupled with the absence of obvious deposits argue against a major contribution to their form via gully incision. If bay formation was initiated by mass wasting or gully incision during the early history of the crater, all evidence has been removed by subsequent, more significant eolian modification.

[36] In summary, the present form of Victoria crater, including bays, capes, rim expression, and presence of interior deposits and dunes, is consistent with considerable, ongoing, eolian degradation and net crater infilling over time. Mass wasting and/or gully incision (by mass wasting or fluvial activity) may contribute to initial evolution of bays but would have been limited mostly to early crater history. Although mass wasting is occurring along the steeper capes, it is facilitated by eolian scour and subsequent disintegration of resulting talus that leaves surfaces steep and exposed. The absence of morphologies (erosional and depositional) associated with noneolian processes implies that any signatures diagnostic of other processes were destroyed by subsequent eolian activity. Therefore, eolian processes are most important in modifying Victoria crater's form and dominate bay evolution, contribute to cape backwasting, have enlarged the crater by $\sim$50 m in alignment with the prevailing winds, and are responsible for crater infilling.

[37] Elsewhere in Meridiani Planum, there are craters (up to 50 km in diameter) that formed during the emplacement of the regional stratigraphy that were buried and subsequently partially exhumed [*Edgett*, 2005]. These craters are typically interbedded within the regional stratigraphy and often retain remnants of the crater-filling deposits. By contrast, Victoria crater postdates local stratigraphy, and there is no evidence of remnant deposits and rocks exposed above the current level of the crater fill. Moreover, given the extreme ease with which the rocks composing Victoria are eroded by the wind, it is difficult to envision its complete or partial exhumation from entombing stratigraphy without more complete destruction of the crater. Hence, we conclude that there is no evidence at Victoria crater suggesting that it was completely filled and subsequently exhumed as suggested by *Edgett* [2005], and there is not any evidence for degradation by water-related processes.

7. Origin of the Annulus

[38] The dark-toned annulus surrounding Victoria is remarkably free of outcrop or blocks (Figure 10) and reaches an average of 590 m from the edge of the raised rim or 760 m from the rim crest. The annulus is somewhat asymmetrical in extent (ranges from 300 to 930 m from the raised rim or from 470 to 1100 m beyond the rim crest), extending farthest to the southwest and northeast (Figure 2). As noted in section 3, the approximate centering of the annulus around Victoria crater suggests that its origin could be related to formation of the crater and may mark the distribution of surrounding ejecta deposits. If originally related to the ejecta deposit, however, the paucity of exposed blocks requires mantling by drift or partial to complete erosion (perhaps along with underlying bedrock disrupted during ejecta emplacement) to account for its present appearance. Conversely, the annulus could be unrelated to the crater and may correspond to a regional geologic or geomorphic contact.

[39] Several characteristics of the annulus link its origin to that of the crater. Because the annulus surrounds the crater, lacks the bedrock outcrops characterizing surround-

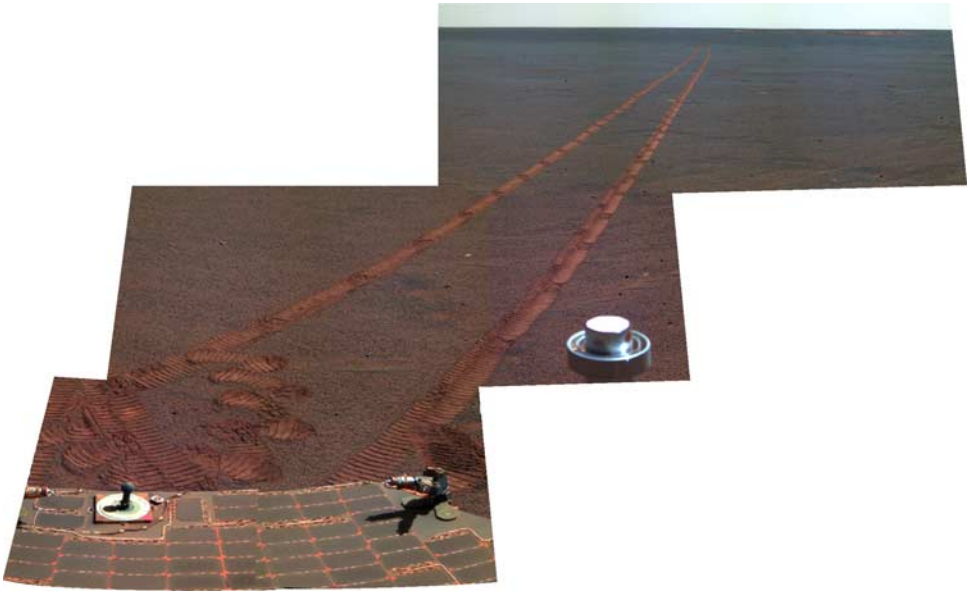

Figure 10. View along the Opportunity rover's (NW to SE) traverse across the annulus surrounding Victoria crater. Image taken near the small crater Emma Dean reveals that the annulus is very low relief and that very few rocks protrude from the mostly hematite spherule–covered surface (Figure 11). Rover tracks are approximately 1 m apart. Approximate true color Pancam mosaic created using sequence p2375 and L257 filters (RGB = 753, 535, and 432 nm) on sol 935 of Opportunity's mission.

ing surfaces, and is marked by a boundary across which there is little observed relief (at least where crossed by the rover on the northwest margin), an origin related to a regional geologic or geomorphic boundary or localized, increased erosion seems coincidental and unrelated to the geology observed by Opportunity during its traverse to Victoria. More likely, the annulus is the modified expression of the ejecta from Victoria, and its average extent is somewhat greater than what is expected for a crater originally 600 m or slightly larger in diameter [*Wilhelms*, 1987]. On the basis of an original crater diameter of 600 m, material would have been excavated from approximately one third to one half the depth of the transient crater [*Melosh*, 1989] or ~60–90 m from equation (2). Nevertheless, the annulus surface displays minimal variability along Opportunity's traverse, suggesting that ejecta excavated from greatest depths were broadly similar in physical properties to those nearer the surface or that such differences are masked by subsequent erosion.

[40] Because the crater and exposed rocks within it are efficiently eroded by eolian processes, it is reasonable to expect that the ejecta deposit surrounding the crater was also readily eroded. The diminished expression of the rim, the planed-off appearance of the near-rim ejecta, paucity of exposed blocks, and occurrence of wind streaks [*Geissler et al.*, 2008] support this contention and are consistent with erosion of nearby craters [*Grant et al.*, 2006; *Golombek et al.*, 2006b]. Eolian erosion, probably accomplished by transported basaltic sand [*Sullivan et al.*, 2005; *Sullivan et al.*, 2007; *Geissler et al.*, 2008], planes off exposed ejecta blocks, leaving behind a lag of resistant hematite spherules that accumulate (Figure 11), trap some of the basaltic sand, and slow additional erosion [*Sullivan et al.*, 2007]. Exposures into the ejecta near the rim crest and at small craters

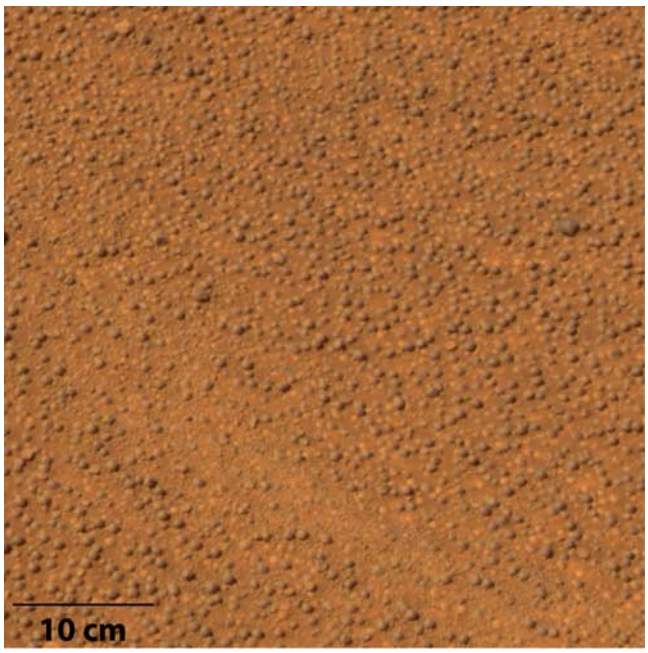

Figure 11. View of the annulus surface near the small crater Emma Dean that reveals that the surface is armored by a lag of hematite spherules that are typically larger and more numerous than those seen on surfaces farther from Victoria crater [*Weitz et al.*, 2006; *Sullivan et al.*, 2007]. The annulus likely reflects the extent of Victoria's ejecta and was created after eolian deflation of soft sulfate rocks left a lag of more resistant spherules that trapped sand and armored the surface against additional erosion [*Sullivan et al.*, 2007]. Approximate true color Pancam image from sequence p2571 using L257 filters (RGB = 753, 535, and 432 nm) on sol 935 of Opportunity's mission.

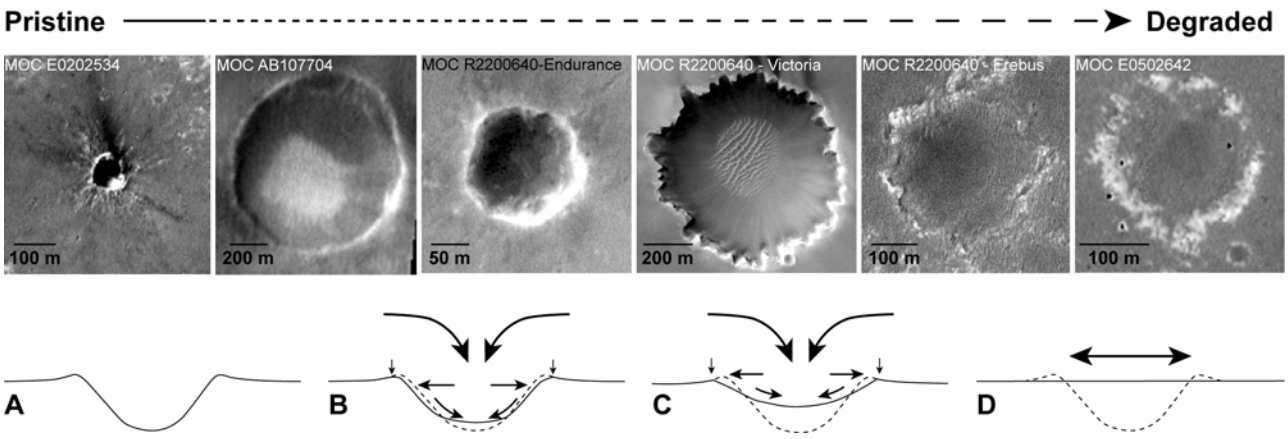

Figure 12. Idealized crater degradation sequence and representative examples for craters within a 2° latitude by 2° longitude area centered on Victoria crater. Pristine craters (stage A) are initially modified by backwasting by mass wasting and eolian activity that is accompanied by infilling as sediments transported across the plains are blown into the crater (stage B). As degradation progresses, mass wasting on the walls becomes less important and walls continue to backwaste by mostly eolian erosion while infilling continues (stage C). Eventually, the walls and rim are eroded to forms presenting little cross section to the prevailing winds, thereby making infilling relatively more important over time and causing the crater to slowly fill to the level of the surrounding plains (stage D). Idealized profiles include approximately 4× vertical exaggeration.

visited while crossing the annulus indicate that the lag of sand and spherules is very thin and no more than ~10–20 cm thick in most locations.

[41] Persistence of the annulus to greater than the expected 1*D* limit (to the southwest and northeast) suggests that the lag is formed after minimal erosion (~1 m or less), consistent with what has been estimated for accumulation of spherules elsewhere along Opportunity's traverse [*Golombek et al.*, 2006b]. More erosion of the thin discontinuous and distal continuous ejecta would remove the distal ejecta completely and lead to lesser extent of the annulus. Nevertheless, along higher-relief surfaces such as the exposed crater rim, erosion can be considerably greater and is consistent with the slope-dependent nature of erosion observed at Meteor Crater on the Earth [*Grant and Schultz*, 1993b]. For example, if Victoria was originally 600 m across, then an average of 3–6 m of vertical erosion of the ejecta deposit has occurred at the present rim. This contrasts with the ~1 m erosion inferred for more distal, lower-relief ejecta surfaces. Greater erosion of the rim is expected because the resistant hematite spherules would be less likely to accumulate on the slightly steeper, higher-relief surfaces versus the lower-relief ejecta beyond. Moreover, the exposed setting of the raised rim suggests that the more resistant spherules could be broken down more rapidly than on the lower-relief, surrounding annulus. Hence, greater predicted erosion of the raised rim likely reflects the evolving nature of the lag on higher-relief, more exposed surfaces rather than a fundamental difference in evolution as compared to more distal ejecta and annulus surfaces. Finally, erosion of 3–6 m near the rim but less than 1 m on more distal ejecta deposits is consistent with estimates of erosion for smaller impact craters and Meridiani Planum in the Amazonian [*Golombek et al.*, 2006b].

[42] The asymmetrical outline of the annulus (Figure 2) could reflect the primary distribution of Victoria's ejecta as a result of an oblique impact [e.g., *Gault and Wedekind*, 1978; *Schultz and Gault*, 1979; *Schultz*, 1992; *Pierazzo and Melosh*, 2000; *Herrick and Hessen*, 2006]. The minimum preserved extent is to the northwest and southeast of the crater, however, and is approximately aligned with the prevailing wind directions [e.g., *Sullivan et al.*, 2005; *Jerolmack et al.*, 2006], which is consistent with enhanced erosion of an initially blocky surface in those directions.

8. Crater Degradation Sequence for Meridiani Planum

[43] Degradation of Victoria crater by mostly eolian processes is dominated by net infilling over time and is consistent with inferences drawn from other craters visited by Opportunity on Meridiani Planum [*Grant et al.*, 2006; *Golombek et al.*, 2006b]. Armed with that information and on the basis of the range of crater morphologies observed in situ, a review of all craters within a 2° latitude by 2° longitude box centered on Victoria was undertaken using narrow-angle orbital images from the Mars Orbiter Camera with the goal of establishing a general crater degradation sequence (Figure 12). This sequence can then be compared to the degradation sequence defined for local, smaller craters on the basis of direct observation along Opportunity's traverse [*Golombek et al.*, 2006b] and models for crater degradation applied to the Sinus Sabaeus region to the east of Meridiani Planum [*Forsberg-Taylor et al.*, 2004].

[44] Pristine craters possessing initially steep walls exposing highly fractured rocks are modified by some mass wasting as debris is shed into crater interiors. Accompanying early eolian erosion of walls and the rim is also important, as the weak, exposed lithologies are scoured by saltating sediments eroded from the walls, ejecta, and basaltic sand transported from the surrounding plains (Figure 12). Some of the dark-toned basaltic sand is trapped

within the crater and causes net infilling over time. Stripping of sediments from the rim and ejecta creates a lag of more resistant hematite spherules that traps some of the regional basaltic sands, slows additional erosion, and leads to evolution of a surrounding annulus (Figures 10 and 11).

[45] Continued backwasting of the walls, predominantly by eolian processes, exploits structural weaknesses (e.g., tear faults) that lead to locally faster backwasting and evolution of the alcoves or bays that define the current rim at Victoria crater (Figure 12). Intervening capes evolve as rocks that are more resistant and/or less disrupted by impact or structure are eroded more slowly by the wind, leading to oversteepening and some collapse. Nevertheless, resultant talus is susceptible to scour and leaves the base of most capes generally exposed. As additional sediments are carried into the crater from the surrounding plains, some are swept into dunes, and net infilling begins to outpace backwasting of the walls. Eventually, bays become rounded and smoothed by sediments blowing into and out of the crater, and bay floors evolve into efficient transport surfaces that are only slowly modified by additional erosion (Figure 12). At this stage, ongoing infilling by sediments delivered from outside of the crater becomes relatively more important in modification and leads to slow infilling of the remaining relief.

[46] In their most degraded forms, craters are filled to the level of the surrounding plains, and the surrounding annulus is slowly eroded and fades. At this advanced degradation state, craters are marked only by outcrops indicating what remains of their rims since they eroded to the level of the plains. With time, even these outcrops, which may be less resistant than the hematite spherule–rich lags on surrounding surfaces, are eroded and thinly covered. As with the annulus at Victoria, however, these outcrops may lie only tens of centimeters below the surface and could be exhumed and further eroded in concert with the surrounding plains.

[47] The sequence described above is largely consistent with that inferred from observation of small craters along Opportunity's traverse [*Golombek et al.*, 2006b] and from models for eolian erosion of craters in Sinus Sabaeus [*Forsberg-Taylor et al.*, 2004] and implies that processes responsible for degrading Victoria and nearby craters are typical for regional surfaces in Meridiani Planum. There is no evidence that the craters explored to date experienced modification by water erosion or that any were filled and subsequently exhumed [*Edgett*, 2005]. Additional erosion is tied to the long-term denudation and lowering of the surrounding plains.

[48] **Acknowledgments.** The authors heartily thank the MER project for their expertise in the design and operation of such capable rovers. Constructive reviews by Jim Rice and Brad Thomson helped to improve the paper. The work described herein was supported by the National Aeronautics and Space Administration.

References

Barlow, N. G. (2005), A review of Martian impact crater ejecta structures and their implications for target properties, in *Large Meteorite Impacts III*, edited by T. Kenkmann, F. Hörz, and A. Deutsch, *Spec. Pap. Geol. Soc. Am.*, *384*, 433–442.

Edgett, K. E. (2005), The sedimentary rocks of Sinus Meridiani: Five key observations from data acquired by the Mars Global Surveyor and Mars Odyssey orbiters, *Mars*, *1*, 5–58, doi:10.1555/mars.2005.0002.

Forsberg-Taylor, N. K., A. D. Howard, and R. A. Craddock (2004), Crater degradation in the Martian highlands: Morphometric analysis of the Sinus Sabaeus region and simulation modeling suggest fluvial processes, *J. Geophys. Res.*, *109*, E05002, doi:10.1029/2004JE002242.

Garvin, J. B., S. E. H. Sakimoto, J. J. Frawley, and C. Schnetzler (2000), North polar region craterforms on Mars: Geometric characteristics from the Mars Orbiter Laser Altimeter, *Icarus*, *144*, 329–352, doi:10.1006/icar.1999.6298.

Garvin, J. B., S. E. H. Sakimoto, and J. J. Frawley (2003), Craters on Mars: Global geometric properties from gridded MOLA topography, paper presented at Sixth International Conference on Mars, Lunar and Planet. Inst., Pasadena, Calif.

Gault, D. E. (1970), Impact cratering, in *A Primer in Lunar Geology*, edited by R. Greeley and P. H. Schultz, pp. 137–175, NASA Ames Res. Cent., Moffett Field, Calif.

Gault, D. E., and J. A. Wedekind (1978), Experimental studies of oblique impact, *Proc. Lunar Planet. Sci. Conf.*, *9th*, 3843–3875.

Gault, D. E., W. L. Quaide, and V. R. Oberbeck (1968), Impact cratering mechanisms and structures, in *Shock Metamorphism of Natural Materials*, edited by B. M. French and N. M. Short, pp. 87–100, MonoBooks, Baltimore, Md.

Geissler, P. E., et al. (2008), First in situ investigation of a dark wind streak on Mars, *J. Geophys. Res.*, *113*, E12S31, doi:10.1029/2008JE003102.

Golombek, M. P., et al. (2006a), Geology of the Gusev cratered plains from the Spirit rover transverse, *J. Geophys. Res.*, *111*, E02S07, doi:10.1029/2005JE002503.

Golombek, M. P., et al. (2006b), Erosion rates at the Mars Exploration Rover landing sites and long-term climate change on Mars, *J. Geophys. Res.*, *111*, E12S10, doi:10.1029/2006JE002754.

Grant, J. A. (1999), Evaluating the evolution of process specific degradation signatures around impact craters, *Int. J. Impact Eng.*, *23*, 331–340, doi:10.1016/S0734-743X(99)00084-6.

Grant, J. A., and P. H. Schultz (1993a), Degradation of selected terrestrial and Martian impact craters, *J. Geophys. Res.*, *98*, 11,025–11,042, doi:10.1029/93JE00121.

Grant, J. A., and P. H. Schultz (1993b), Erosion of ejecta at Meteor Crater, Arizona, *J. Geophys. Res.*, *98*, 15,033–15,047, doi:10.1029/93JE01580.

Grant, J. A., C. Koeberl, W. U. Reimold, and P. H. Schultz (1997), Gradation of the Roter Kamm impact crater, Namibia, *J. Geophys. Res.*, *102*, 16,327–16,388, doi:10.1029/97JE01315.

Grant, J. A., et al. (2006), Crater gradation in Gusev crater and Meridiani Planum, Mars, *J. Geophys. Res.*, *111*, E02S08, doi:10.1029/2005JE002465.

Grant, J. A., S. A. Wilson, B. A. Cohen, M. P. Golombek, P. E. Geissler, R. S. Sullivan, and R. L. Kirk (2008), Degradational modification of Victoria crater, Mars, *Lunar Planet Sci.*, *XXXIX*, abstract 1878.

Herrick, R. R., and K. K. Hessen (2006), The planforms of low-angle impact craters in the northern hemisphere of Mars, *Meteorit. Planet. Sci.*, *41*, 1483–1495.

Hurst, M., M. P. Golombek, and R. Kirk (2004), Small crater morphology within Gusev crater and Isidis Planitia: Evidence for widespread secondaries on Mars, *Lunar Planet. Sci.*, *XXXV*, abstract 2068.

Jerolmack, D. J., D. Mohrig, J. P. Grotzinger, D. A. Fike, and W. A. Watters (2006), Spatial grain size sorting in eolian ripples and estimation of wind conditions on planetary surfaces: Application to Meridiani Planum, Mars, *J. Geophys. Res.*, *111*, E12S02, doi:10.1029/2005JE002544.

Malin, M. C., and K. S. Edgett (2000), Evidence for recent groundwater seepage and surface runoff on Mars, *Science*, *288*, 2330–2335, doi:10.1126/science.288.5475.2330.

McEwen, A. S., B. S. Preblich, E. P. Turtle, N. A. Artemieva, M. P. Golombek, M. Hurst, R. L. Kirk, D. M. Burr, and P. R. Christensen (2005), The rayed crater Zunil and interpretations of small impact craters on Mars, *Icarus*, *176*, 351–381, doi:10.1016/j.icarus.2005.02.009.

McEwen, A. S., et al. (2007), Mars Reconnaissance Orbiter's High Resolution Imaging Science Experiment (HiRISE), *J. Geophys. Res.*, *112*, E05S02, doi:10.1029/2005JE002605.

McGetchin, T. R., M. Settle, and J. W. Head (1973), Radial thickness variation in impact crater ejecta: Implications for lunar basin deposits, *Earth Planet. Sci. Lett.*, *20*, 226–236, doi:10.1016/0012-821X(73)90162-3.

Melosh, H. J. (1989), *Impact Cratering*, 245 pp., Oxford Univ. Press, New York.

Moore, H. J., C. A. Hodges, and D. H. Scott (1974), Multi-ringed basins—Illustrated by Orientale and associated features, *Proc. Lunar Planet. Sci. Conf.*, *5th*, 71–100.

Okubo, C. H. (2007), Strength and deformability of light-toned layered deposits observed by MER Opportunity: Eagle to Erebus craters, Mars, *Geophys. Res. Lett.*, *34*, L20205, doi:10.1029/2007GL031327.

Pelletier, J. D., K. J. Kolb, A. S. McEwen, and R. L. Kirk (2008), Recent bright gully deposits on Mars: Wet or dry flow?, *Geology*, *36*, 211–214, doi:10.1130/G24346A.1.

Pierazzo, E., and H. J. Melosh (2000), Understanding oblique impacts from experiments, observations, and modeling, *Annu. Rev. Earth Planet. Sci.*, *28*, 141–167, doi:10.1146/annurev.earth.28.1.141.

Pike, R. J. (1977a), Size dependence of fresh impact craters on the Moon, in *Impact and Explosion Cratering*, edited by D. J. Roddy et al., pp. 489–509, Pergamon, New York.

Pike, R. J. (1977b), Apparent depth/apparent diameter relation for lunar craters, in *Proceedings of the Eighth Lunar Science Conference*, vol. 3, *Planetary and Lunar Surfaces*, edited by R. B. Merill et al., pp. 3427–3436, Pergamon, New York.

Pike, R. J. (1980), *Geometric Interpretation of Lunar Craters*, *U.S. Geol. Surv. Prof. Pap.*, *1046-C*, 77 pp.

Pike, R. J., and D. E. Wilhelms (1978), Secondary-impact craters on the Moon: Topographic form and geologic process, *Lunar Planet. Sci.*, *IX*, 907–909.

Quaide, W. L., and V. R. Oberbeck (1968), Thickness determinations of the lunar surface layer from lunar impact craters, *J. Geophys. Res.*, *73*, 5247–5270, doi:10.1029/JB073i016p05247.

Ritter, D. F., R. C. Kochel, and J. R. Miller (1995), *Process Geomorphology*, 540 pp., Wm. C. Brown, Dubuque, Iowa.

Roddy, D. J. (1978), Pre-impact geologic conditions, physical properties, energy calculations, meteorite and initial crater dimensions and orientations of joints, faults, and walls at Meteor Crater, Arizona, *Proc. Lunar Planet. Sci. Conf.*, *9th*, 3891–3930.

Roddy, D. J., J. M. Boyce, G. W. Colton, and A. L. Dial Jr. (1975), Meteor Crater, Arizona, rim drilling with thickness, structural uplift, diameter, depth, volume, and mass-balance calculations, *Proc. Lunar Sci. Conf.*, *6th*, 2621–2644.

Schultz, P. H. (1992), Atmospheric effects on ejecta emplacement, *J. Geophys. Res.*, *97*, 11,623–11,662.

Schultz, P. H., and D. E. Gault (1979), Atmospheric effects on Martian ejecta emplacement, *J. Geophys. Res.*, *84*, 7669–7687.

Shoemaker, E. M., and S. W. Kieffer (1974), *Guidebook to the Geology of Meteor Crater, Arizona*, publ. 17, 66 pp., Cent. for Meteorite Stud., Ariz. State Univ., Tempe.

Soderblom, L. A., et al. (2004), Soils of Eagle crater and Meridiani Planum at the Opportunity rover landing site, *Science*, *306*, 1723–1726, doi:10.1126/science.1105127.

Squyres, S. W., et al. (2004), The Opportunity rover's Athena science investigation at Meridiani Planum, Mars, *Science*, *306*, 1698–1703, doi:10.1126/science.1106171.

Sullivan, R., et al. (2005), Aeolian processes at the Mars Exploration Rover Meridiani Planum landing site, *Nature*, *436*, 58–61, doi:10.1038/nature03641.

Sullivan, R., R. E. Arvidson, J. Grotzinger, A. Knoll, M. Golombek, B. Jolliff, S. Squyres, and C. Weitz (2007), Aeolian geomorphology with MER Opportunity at Meridiani Planum, Mars, *Lunar Planet. Sci.*, *XXXVIII*, abstract 2048.

Turner, A. K., and R. L. Schuster (Eds.) (1996), Landslides: Investigation and mitigation, *Spec. Rep. 247*, 675 pp., Transp. Res. Board, Natl. Res. Counc., Washington, D. C.

Varnes, D. J. (1978), Slope movement types and processes, in *Landslides: Analysis and Control*, edited by R. L. Schuster, and R. J. Krizek, *Spec. Rep. 176*, pp. 11–33, Transp. Res. Board, Natl. Res. Counc., Washington, D. C.

Weitz, C. M., R. C. Anderson, J. F. Bell III, W. H. Farrand, K. E. Herkenhoff, J. R. Johnson, B. L. Jolliff, R. V. Morris, S. W. Squyres, and R. J. Sullivan (2006), Soil grain analyses at Meridiani Planum, Mars, *J. Geophys. Res.*, *111*, E12S04, doi:10.1029/2005JE002541.

Wilhelms, D. E. (1987), *The Geologic History of the Moon*, *U.S. Geol. Surv. Prof. Pap.*, *1348*, 302 pp.

Yen, A. S., et al. (2005), An integrated view of the chemistry and mineralogy of Martian soils, *Nature*, *436*, 49–54, doi:10.1038/nature03637.

B. A. Cohen, Marshall Space Flight Center, Mail Code VP40, Huntsville, AL 35812, USA.

P. E. Geissler and R. L. Kirk, U.S. Geological Survey, 2255 North Gemini Drive, Flagstaff, AZ 86001, USA.

M. P. Golombek and T. J. Parker, Jet Propulsion Laboratory, California Institute of Technology, Pasadena, CA 91109, USA.

J. A. Grant and S. A. Wilson, Center for Earth and Planetary Studies, National Air and Space Museum, Smithsonian Institution, Washington, DC 20560, USA. (grantj@si.edu)

R. J. Sullivan, Department of Astronomy, Cornell University, 308 Space Sciences Building, Ithaca, NY 14853, USA.